

In vivo comparison of 2D and 3D T_2^* in the rat lung using hyperpolarized helium-3 MRI at 1.5 T

K. Hill^{1,2}, J.-M. Pérez-Sánchez², R. Santarelli², M. Sarracanie², P. Hagot², M. Friese², X. Maître², and L. Darrasse²

¹University of Oxford, Oxford, Oxfordshire, United Kingdom, ²Imagerie par Résonance Magnétique Médicale et Multimodalité (UMR 8081), Univ Paris-Sud, CNRS, Paris, Le Kremlin-Bicêtre, France

Introduction

The transverse relaxation time, T_2^* , of hyperpolarized helium-3 in the lungs is a measure of the MR signal duration and it is an important parameter for pulse sequence optimization and image contrast. The T_2^* has also shown promise in characterizing lung microstructure due to its sensitivity to local gradients caused by gas-tissue interfaces, whose abundance per unit volume changes with lung inflation and pathological modification [1,2,3]. Despite the lung's three-dimensional, folded, extensible structure, most measurements of helium-3 T_2^* have been performed using 2D projection imaging which inherently neglects the effects of the complex microstructure on T_2^* . This work uses five rats *in vivo* to compare the T_2^* in a 2D projection image with true 3D imaging with 3, 6, and 12 slices.

Materials and Methods

Transverse relaxation times of the hyperpolarized helium-3 signal in rat lungs *in vivo* were measured at 1.5 T (Achieva[®], Philips Medical Systems, The Netherlands) at CIERM, Hôpital Bicêtre, Paris. The helium-3 gas was polarized onsite using a custom-built metastability exchange optical pumping system which provided a polarization of ~10%. Five Wistar rats, with masses ranging from 250 g to 270 g, were anesthetized using a solution of ketamine (80 mg/kg) and xylazine (10 mg/kg), tracheotomized, and successively placed at the center of an 84 mm diameter Helmholtz coil with a quality factor of 400. After administration of 7 mL of helium-3, a multi-echo FLASH sequence was used to acquire 2D projection images (four echoes) and 3D images (two echoes) with 3, 6, and 12 coronal slices and interleaved echo times of $TE = \{1.88, 10.88\}$ ms (3D) and $TE = \{1.88, 8.88, 15.88, 22.88\}$ ms (2D). The sequence parameters were as follows: FOV=64×56 mm², matrix=32×28, TR/TE₁=24/1.88 ms, BW=1360 Hz/pixel, $\alpha=1.3^\circ$. SNR was calculated by averaging the real and imaginary noise and the images were thresholded using a 5 σ mask to localize the lungs. Magnetization loss due to RF depolarization was corrected using a B_1 map and the T_2^* maps were computed using an exponential fit on a voxel-per-voxel basis.

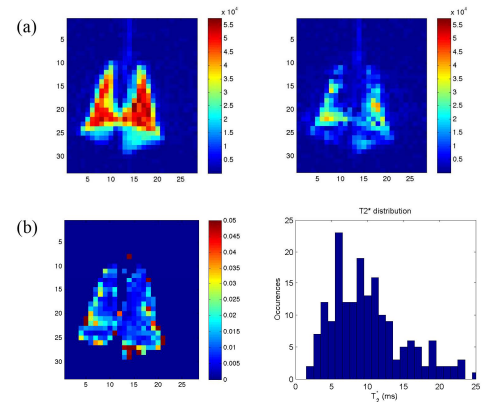


Figure 1: (a) Images from a double-echo sequence. $TE_1 = 1.88$ ms (left), $TE_2 = 10.88$ ms (right), and voxel size = $2 \times 2 \times 4$ mm³. (b) Corresponding T_2^* map and histogram. Median $T_2^* = 10$ ms.

Results

Figure 1 shows images from a double-echo 3D sequence with voxel size $2 \times 2 \times 4$ mm³. 1(a) shows the magnitude data for $TE_1 = 1.88$ ms (left) and $TE_2 = 10.88$ ms (right), while 1(b) shows the corresponding T_2^* map and histogram with median $T_2^* = 10$ ms. Figure 2 shows the mean T_2^* over four rats for three central slices (8, 9, and 10) from a 3D acquisition with voxel size = $2 \times 2 \times 2$ mm³. The slices were chosen due to their high SNR. A Wilcoxon rank sum test compared the means of each slice and statistically significant differences were found between slices 8 and 10 ($p = 0.02$) and slices 9 and 10 ($p = 0.03$), as well as a noteworthy but insignificant difference between slices 8 and 9 ($p = 0.06$). Figure 3 shows two T_2^* maps from a rat that had ventilation defects in the central region of its left lung. The asymmetry between the left and right lung are observable in the T_2^* map corresponding to the $2 \times 2 \times 2$ mm³ slice but not in the T_2^* map from the projection image. T_2^* values shown here are of similar magnitudes to those found in the literature.

3D T_2^* values per slice with $2 \times 2 \times 2$

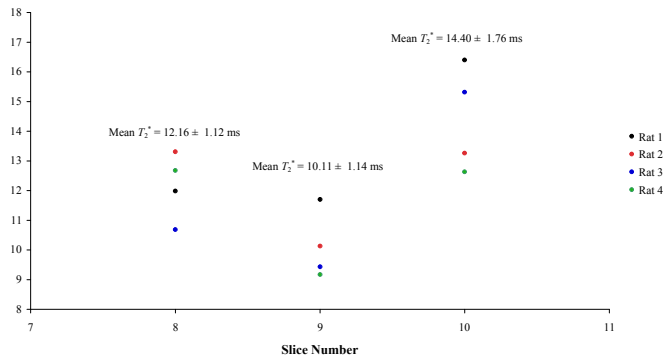


Figure 2: Mean T_2^* value for selected slices (with high SNR) in a 3D image with voxel size = $2 \times 2 \times 2$ mm³. The data points for each slice correspond to four rats with images acquired *in vivo*.

Discussion

This work represents a direct comparison of T_2^* relaxation times in 2D and in 3D with varying slice size. The results in Figure 2 and Figure 3 clearly show that 3D imaging offers a superior ability to detect statistically different local phenomena that may not be apparent in a 2D projection image. Differences between the T_2^* value in each 3D slice, as shown in Figure 2, may be partly gravitational, as proposed for apparent diffusion coefficient differences [4], and may also be related to increased blood perfusion in posterior slices. The T_2^* maps shown in Figure 3 have different lung shapes owing to their origin: the 3D slice represents the lung structure at the particular (central) region while the 2D projection offers a compressed picture of the whole lung. It is clear that T_2^* maps yield similar information to apparent diffusion coefficient (ADC) maps [5] with potential higher sensitivity, and further studies are needed to determine whether T_2^* can be effectively used as a diagnostic tool for measuring changes in the lung microstructure.

References

1. X.J. Chen *et al.* Magn. Reson. Med., 42(4):729-737, 1999.
2. L. de Rochefort *et al.*, Proc 11th ISMRM, 2004, p. 2724.
3. S. Ajaoui *et al.*, Proc 15th ISMRM, 2008, p. 2652.
4. Fichele *et al.*, J. Magn. Reson. Imaging, 2004, 20(2):331-335.
5. S. Ajaoui *et al.*, Proc ESMRMB 2009.

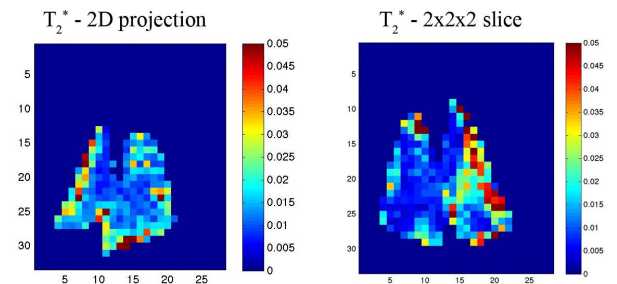


Figure 3: Two T_2^* maps of the same rat which had a ventilation defect in the central region of its left lung. The T_2^* map from the projection image shows little indication of the ventilation defect while the $2 \times 2 \times 2$ T_2^* map clearly shows the local defect.